Varying-Time Random Effects Models for Longitudinal Data: Spatial Disaggregation and Temporal Interpolation of Remote Sensing Data

Hervé Cardot, Philippe Maisongrande, Robert Faivre

Varying-Time Random Effects Models for Longitudinal Data: Spatial Disaggregation and Temporal Interpolation of Remote Sensing Data

Hervé Cardot[1], Philippe Maisongrande[2] and Robert Faivre[1]
(1) INRA Toulouse, Unité Biométrie et Intelligence Artificielle
31326 Castanet-Tolosan, Cedex, FRANCE
(2) CNES at Centre D'Etudes Spatiales de la Biosphère, UMR CNES-CNRS,
18 Av. Edouard Belin, 31401 Toulouse, France.
e-mail: herve.cardot@enesad.inra.fr, philippe.maisongrande@cesbio.cnes.fr,
robert.faivre@toulouse.inra.fr

10 novembre 2005

Résumé

Remote sensing is an helpful tool for crop monitoring or vegetation growth estimation at a country or regional scale. However, satellite images generally have to cope with a compromise between the time frequency of observations and their resolution (*i.e.* pixel size). When concerned with high temporal resolution, we have to work with information on the basis of kilometric pixels that represent aggregated responses of multiple land cover inside each low resolution pixel. Disaggreggation is then necessary to downscale from the square kilometer to the local dynamic of each parcel (crop, wood, meadows,...).

We propose to address this question through the generalisation of varying-time regression models for longitudinal data and/or functional data by introducing local mixed effects. The estimators are built by expanding the mixed pixels trajectories with B-splines functions and maximizing the log-likelihood with a Backfitting-ECME algorithm. A BLUP formula allows then to get the "best possible" estimations of the local temporal responses of each crop when observing mixed pixels trajectories. We show that this model has many potential applications in remote sensing and an interesting one consists in coupling high and low spatial resolution images in order to perform temporal interpolation of high spatial resolution images (20m), increasing the knowledge on particular crops in very precise locations.

The disaggregation, or downscaling, and interpolation approaches

are illustrated on remote sensing data obtained on the South-Western of France during the year 2002.

keywords : Backfitting, BLUP, covariance function, downscaling, ECME, functional data, mixed effects, mixed pixels, splines, unmixing, SPOT/VGT, SPOT/HRVIR, remote sensing.

1 Introduction

Observation of the Earth with satellites has given rise to much attention for several decades since satellite images allow to deduce important information about the state and the evolution of characteristic of the earth. Remote sensing has been used successfully (see *e.g.* the web sites `http ://www.noaa.gov/eos.html` and `http ://www.eumetsat.int/`) in many fields of science (meteorological patterns, deforestation, desert advances, ...).

The satellite imagery is based on the same principle as classical digital cameras used everyday to make pictures (Richards & Jia, 2005). Each pixel of the image corresponds to the amount of energy that each cell of a CCD (the retina of the sensor) receives. The optical sensor (or camera) makes images of energy reflected by the target. It is very common in remote sensing to manipulate the notion of reflectance which is simply the energy reflected by the target normalised by the incident energy. Measured at different wavelengths, reflectances provide information on the spectral response of surfaces. Considering for example the vegetation, the greeness of continental surfaces can be monitored along time with Vegetation Indices, VIs, based on the difference between reflectances measured in the red part of the spectrum (where green leaves absorb a lot) and near infra red part where leaves reflectances are much higher. Among the possible environmental applications of optical remote sensing, we have chosen to devote this study to the crop monitoring at a regional scale, and more specifically to the estimation of local crops responses along time. Such an objective requires High Resolution information at least once a week.

Yet, among optical sensors that currently operate on low orbit (around 800km), one can distinguish 2 major families in term of spatial resolution and time frequency of observation. The first group is composed of low and medium spatial resolution sensors, whose pictures elementary units (pixels) respectively represent areas ranging between 1km by 1km and 250m by 250m. This type of sensors provide users with a costless daily global coverage of the earth. The other group is composed of High Resolution missions, which deliver very accurate spatial information (a pixel representing a sur-

face ranging from 5m×5m to 20m×20m) but sparse temporal repetition (generally less than one image per month) and with a relatively high cost for the users.

Thus, the only way to get temporal information is to consider time series of low resolution images at the expense of a loss of accuracy of the (spatial) information which is aggregated.

The spatial aggregation problem is described in Figure (1) which presents the same area observed both with sensors at high and low spatial resolutions. For example, in the visible and the near infra-red wavelengths, onboard the 2 last spot satellites SPOT 4 and SPOT 5, a daily global coverage of continental surfaces is made possible at kilometric resolution thanks to the VEGETATION sensor (at the top in Figure 1). On the same platform, the HRVIR (High Resolution) sensor provides users with regional scenes (60km×60km) at 20m resolution but its repetitiveness of observation on a specific region reaches hardly one available image per month (Coret *et al.* 2005). This means that frequent images are only made available on the basis of kilometric pixels that represent aggregated responses of multiple land cover inside each low resolution pixel. Figure (1) shows that aggregation induces a non negligible amount of loss of spatial information and, as a consequence, a loss of precision on the crop development in each plot. Disagreggation is then necessary to downscale from the square kilometer to the local dynamic of each parcel (crop, wood, meadows,...). In this case, the downscaling or disaggregation problem consists in recovering the local trajectories knowing the noisy aggregated response and the proportions of land surface of the different themes within a mixed pixel. We may expect to get accurate enough estimations of these local behavior by taking into account the *temporal evolution* of the aggregated trajectories.

Here, we address this downscalling issue on the basis of a natural statistical model relying on mixed effects for longitudinal data (Laird & Ware, 1982). This model is a direct extension to longitudinal (Diggle *et al.* 1994) and functional data (Rice 2004, Ramsay & Silverman, 2005) of a previous work by Faivre & Fischer (1997) who considered the downscaling problem for only one image, that is to say at one date, and thus without taking into account the temporal structure of the correlation. Our approach allows to take implicitly into account the spatial and temporal variations of the different responses without having to assume explicitly any kind of spatial correlation that would lead to intractable estimation procedures.

Although parametric growth models exist for some specific crops, they are not available for most of the themes under studies. Furthermore, these parametric models are nonlinear and the existing estimation procedures for

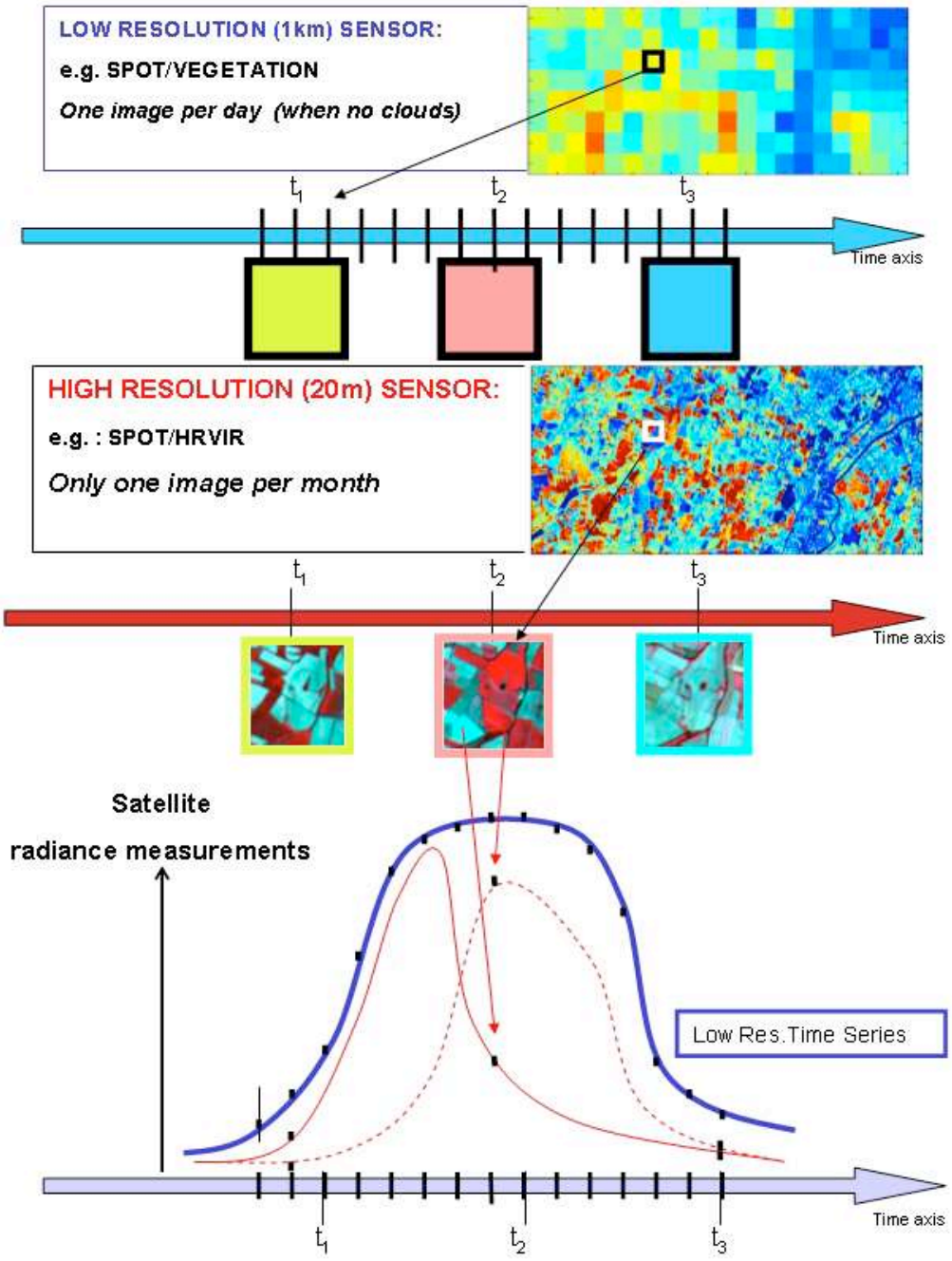

FIG. 1 – With satellite images, technical constrains oblige to choose between repetitiveness and pixels resolution. We present, along time, a same scene observed at two different resolution and repetitiveness. On top, the temporal evolution observed by the Low Resolution Sensor SPOT4/VGT at many frequent dates (potentially 1 image per day). The bottom part shows sparse time series of three high resolution images acquired by SPOT4/HRVIR (hardly available once per month). Length of the time axis is about one year.

nonlinear mixed effects models are nowadays still not efficient enough to cope with such large data sets (see *e.g* Déjean *et al.* 2002). Let us notice that when one has at hand "biophysical" models describing the behavior at a local scale of quantities such as soil moisture combined with auxiliary information such as soil water storage capacity, deterministic procedures combining remote sensing and auxiliary information have been developed successfully for disaggregation (see Pellenq *et al.*, 2003 or Merlin *et al.* 2005).

This is not the case here and we propose a statistical nonparametric approach which appears to be rather simple and well adapted to deal with a huge amount of data. Let us notice that an approach based on local polynomials has been published recently by Wu and Liang (2004) but it does not seem to be suitable for such large remote sensing datasets. We propose to expand the temporal trajectories with B-splines functions which are known to provide both accurate approximations to smooth functions (Dierckx, 1993), which is a natural assumption for phenological curves, and a parsimonious nonparametric model. It is a direct extension of the model studied by Hoover *et al.* (1998) who did not introduce random effects in their varying-time regression model. Our estimation procedure relies on maximizing the log-likelihood function according to the coordinates in the B-splines basis by combining a weighted backfitting procedure (Hastie & Tibshirani, 1990) for the fixed effects and an ECME step (Mac Lachlan & Krishnan, 1997) for the variance components. The proposed algorithm is rather effective and it takes only a few minutes to converge with images representing area of about 4500 km^2 and 35 dates of observation.

To resume, we address in this article, with the same mixed effects model for longitudinal data, the issues of

1. Estimation of the statistical characteristics (mean and variance functions) of the different themes when observing aggregated longitudinal data with known proportions. Downscaling is performed using a BLUP formula to get the best approximation of the individual responses.
2. Temporal interpolation of high resolution remote sensing data when observing both low resolution with a high time frequency and high resolution images at a few different dates (between 3 and 10).

In section 2, we present the aggregation model and give empirical justifications for such a mixed effects approach. Section 3 describes the estimation procedure. In section 4 a brief simulation study confirms the good properties of the B-splines approximation and the optimization algorithm. Section 5 presents a real life application in the South-West of France, a region for which we have, during year 2002, a sequence of 36 medium resolution VEGE-

TATION images as well as 10 SPOT4/HRVIR high resolution images inside an area of about 4500 km^2. Finally, section 6 proposes a general discussion, some extensions of this approach and what could be next investigations.

2 The aggregation model of phenological curves

Before going on, let us fix some notations. We have p low spatial resolution images observed at p different instants during the season, $t_1 < t_2 < \cdots < t_p$, which are not necessarily equi-spaced. Each image is composed of n coarse resolution pixels i, $i = 1, \ldots, n$ from which we get n trajectories associated to the mixed pixels, $\mathbf{X}_i = (X_i(t_1), \ldots, X_i(t_p))'$. We also suppose that the land use is known, that is to say we have the proportion π_{ij} of surface of each theme j, $j = 1, \ldots, J$ within each pixel i.

In the visible and the near infra-red wavelengths, a natural aggregation model (Foody & Cox, 1994) of the responses of the different themes is the following one :

$$X_i(t) = \sum_{j=1}^{J} \pi_{ij}\ \rho_{ij}(t) + \varepsilon_{i,t}, \quad t \in \{t_1, t_2, \cdots, t_p\}, \tag{1}$$

where $\rho_{ij}(t)$ is the reflectance curve, or "phenological curve", or local response for the considered theme j (*e.g.* crop type), within pixel i and the noise $\varepsilon_{i,t}$ are supposed to be independent and drawn from a Gaussian distribution with mean zero and variance σ^2. Let us notice that model (1) only describes the "mean" response $\rho_{ij}(t)$ of plots of crop j within pixel i. Then, it is well adapted for modeling local responses of crops since the intra-pixel variabilities are relatively small compared to the inter (mixed) pixel variabilities. This hypothesis is realistic for remote sensing when dealing with crops and pixels whose size is about 1km^2. Indeed, within such a surface, the assumption of "homogeneity" in the responses of different plots of a same crop is often satisfied.

Unfortunately the parameters of interest $\rho_{ij}(t)$ of model (1) can not be identified when observing the aggregated responses $X_i(t)$. To cope with this problem, Cardot *et al.* (2003) made following simplification

$$\rho_{ij}(t) = \rho_j(t), \quad t \in [0, T], \tag{2}$$

assuming that, for relatively small areas (around 40 km $\times$ 40km), the response of a culture does not vary with the location i of the pixel. One major drawback of this approach is that it does not take into account the local variations of the phenological curves assuming the growth of a culture as being

nearly identical from one location to another. Unfortunately this might not be the case (see next section), even for regions with moderate size, since agricultural practices (irrigation amount, sowing dates, ...) may differ from one farmer to another. Furthermore, factors such as soil composition or climate may also vary spatially, influencing locally the crop development and its temporal evolution. Thus, one has to find an intermediate model between the overparametrized model (1) and the too simple model (2).

2.1 Towards a mixed effects approach

Thanks to a regional scientific project involving the high resolution monitoring of a specific region near Toulouse ("Sud-Ouest" project, see section 5 for more details), we also have a time series of 10 dates of high resolution images (SPOT4/HRVIR) during year 2002. This dataset allows the diagnostic of variations of the responses of each vegetation type around its mean phenological curve.

For instance, let us have a closer look at temporal responses according to the PVI index (Tucker, 1979) of pixels composed only of "wheat crops" (see Figure 2). The PVI index, a linear combination of the responses in the RED and NIR channels defined by PVI=a PIR- b RED with $a = 0.62$ and $b = 0.78$ in this region, shows that assumption (2) is really too strong. One cannot assume that variations of the "wheat" pixel trajectories around its mean phenological curve are only due to independent noises as supposed in 2). Indeed a functional PCA (Ramsay & Silverman, 2005) exhibits a high temporal correlation structure, meaning that the variations around the mean function $\rho_j(t)$ have a strong temporal structure and projecting the data onto a 2-dimensional space allows to explain more than 70 % of the whole variability.

Looking now at the two last displays in Figure (2), in which we have drawn the densities of the principal components, one clearly sees that even if the principal components are not exactly Gaussian they are clearly unimodal and can be approximated, at first sight, without much error, by Gaussian random variables. Having in mind these consideration Cardot, Faivre and Maisongrande (2004) proposed a Gaussian mixed effects model in order to describe the temporal behavior of mixed pixels.

Assuming the response of different crops are independent and that the temporal correlation of crops does not depend on the location, we propose

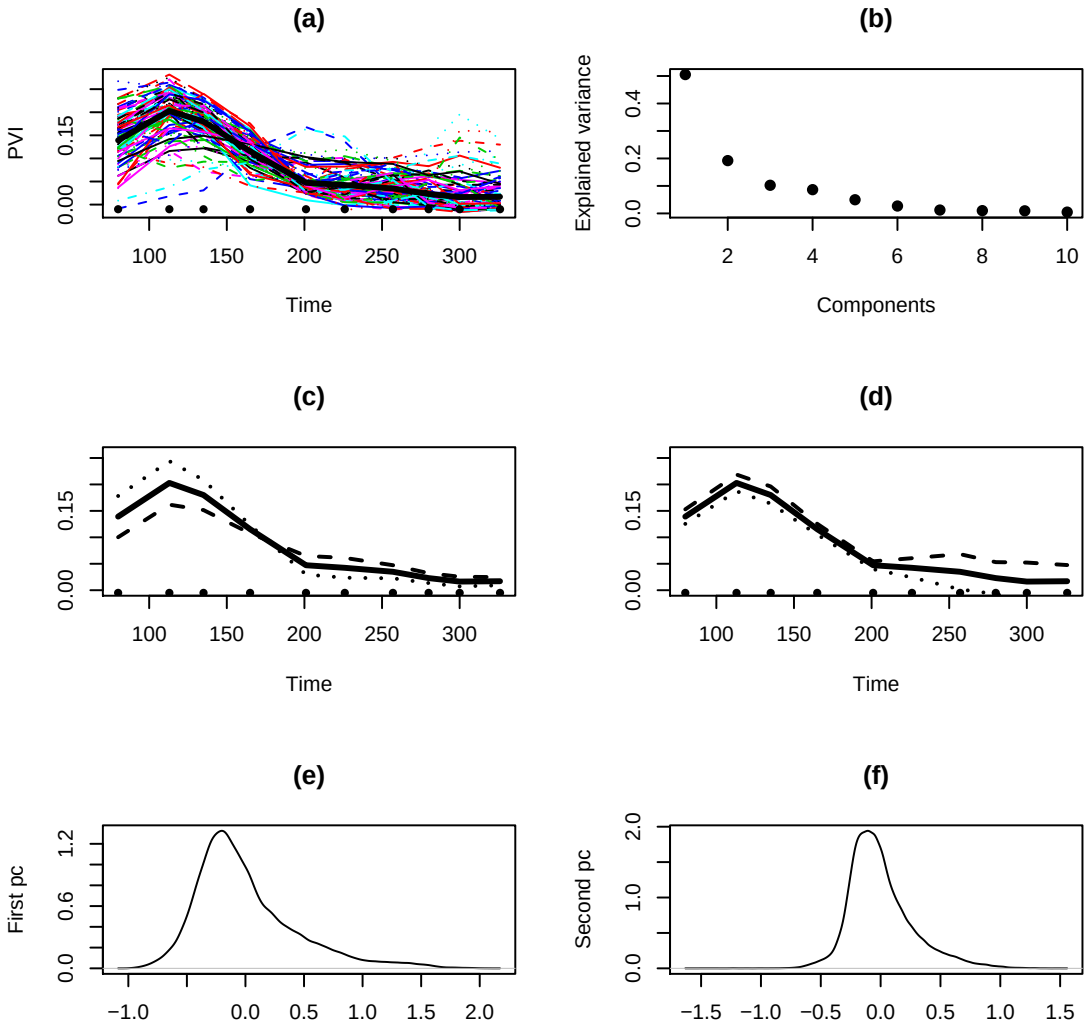

FIG. 2 – Functional Principal Components Analysis of the response of the PVI of high resolution pixels observed at 10 different instants during year 2002 and containing 100 % of the theme "Wheat". The graphs represent a/ a sample of one hundred wheat pixels trajectories, b/ the explained variance by the ten principal components, c/ and d/ the variation around the mean trajectories induced by respectively the first and second eigenfunctions, e/ and f/ the density respectively of the first and second principal components.

the following model

$$\left\{ \begin{array}{rcl} X_i(t) & = & \displaystyle\sum_{j=1}^{J} \pi_{ij}\ \rho_{ij}(t) + \varepsilon_{i,t}, \quad t \in \{t_1, \ldots, t_p\}, \\ \boldsymbol{\rho}_{ij} & \sim & \mathcal{N}\left(\boldsymbol{\rho}_j, \boldsymbol{\Gamma}_j\right), \quad j = 1, \ldots, J, \end{array} \right. \tag{3}$$

where $\rho_j(t)$ is the expectation of the random function $\rho_{ij}(t)$, $\boldsymbol{\rho}_j = (\rho_j(t_1), \ldots, \rho_j(t_p))'$, and $\boldsymbol{\Gamma}_j$ is the covariance matrix with elements

$$[\boldsymbol{\Gamma}_j]_{\ell,\ell'} = \mathrm{cov}(\rho_{ij}(t_\ell), \rho_{ij}(t_{\ell'})) = \gamma_j(t_\ell, t_{\ell'}), \quad \ell, \ell' = 1, \ldots p.$$

The noise components $\varepsilon_{i,t}$ are supposed to be independent and Gaussian with mean zero and variance σ^2. Model (3) is a random effects varying-time regression model.

2.2 Interpolation and prediction with the BLUP formula

Assuming model (3) is true, spatial disaggregation and temporal interpolation can be handled naturally with the BLUP formula (Robinson, 1991) which is recalled now. If $(\mathbf{U}, \mathbf{V})$ is a Gaussian multivariate random variable

$$(\mathbf{U}, \mathbf{V}) \sim N\left(\begin{pmatrix} \boldsymbol{\mu}_u \\ \boldsymbol{\mu}_v \end{pmatrix}, \begin{pmatrix} \boldsymbol{\Gamma}_u & \boldsymbol{\Gamma}_{u,v} \\ \boldsymbol{\Gamma}_{v,u} & \boldsymbol{\Gamma}_v \end{pmatrix}\right)$$

the best linear unbiased prediction of the component $\mathbf{U}$ having observed $\mathbf{V} = \mathbf{v}$, is given by the well known BLUP formula

$$\mathbb{E}\left(\mathbf{U} | \mathbf{V} = \mathbf{v}\right) = \boldsymbol{\mu}_u + \boldsymbol{\Gamma}_{u,v}\boldsymbol{\Gamma}_v^{-1}\left(\mathbf{v} - \boldsymbol{\mu}_v\right)\ . \tag{4}$$

Going back to our study and assuming that $X_i, \pi_{ij}, \boldsymbol{\rho}_j$, $\boldsymbol{\Gamma}_j$ and σ^2 are known, we can give an answer to the first question, that is to say determine the best estimation of the response of a crop within a mixed pixel. Taking $U = \rho_{ij}(t)$ and $\mathbf{V} = \mathbf{X}_i = (X_i(t_1), \ldots, X_i(t_p))'$ we get

$$\mathbb{E}\left(\rho_{ij}(t) \mid \mathbf{X}_i\right) = \rho_j(t) + \mathrm{Cov}(\rho_{ij}(t), \mathbf{X}_i)\mathrm{Var}(\mathbf{X}_i)^{-1}\left(\mathbf{X}_i - \sum_{j=1}^{J} \pi_{ij}\boldsymbol{\rho}_j\right) \tag{5}$$

where

$$\mathrm{Cov}(\rho_{ij}(t), \mathbf{X}_i) = \pi_{ij}\left(\gamma_j(t, t_1), \ldots, \gamma_j(t, t_p)\right)$$

and

$$[\mathrm{Var}(\mathbf{X}_i)]_{\ell,\ell'} = \sigma^2 I_{\{\ell=\ell'\}} + \sum_{j=1}^{J} \pi_{ij}^2 \gamma_j(t_\ell, t_{\ell'})\ .$$

If we now observe a plot with a higher resolution sensor at a few intants $\tau_1, \ldots, \tau_\kappa$ with $\kappa << p$, its temporal trajectory can be approximated (using the best linear approximation) at any other instant τ. Assuming that we also observe during the same period of time (but not necessarily the same instants) the trajectory of the underlying mixed pixel $\mathbf{X}_i = (X_i(t_1), \ldots, X_i(t_p))$, temporal interpolation is performed by applying the BLUP formula (4) with $U = \rho_{ij}(\tau)$ and $\mathbf{V} = \left(\boldsymbol{\rho}_{ij}, \mathbf{X}_i\right)'$.

Note that we can also get the conditional variance both for the interpolation and disagregation approaches.

The next section explain how we can get maximum likelihood estimations of the different parameters of interest.

3 Maximum likelihood estimators

We first propose to expand the observed aggregated trajectories with B-splines basis. Then we can get an approximation to the likelihood function and look for its maximum with an algorithm that combines the Backfitting for the fixed effects and the ECME for the random components.

3.1 Splines approximation of the phenological curves and their conditional variances

Trajectories are expanded in B-splines basis (Dierckx, 1993) in order to have a finite and relatively small number of parameters to estimate. These functions are known to provide parsimonious and good approximations to "smooth functions" such as the true phenological curves. To gain in flexibility, we consider two different basis for the mean phenological curves and for the individual variations. We take a B-splines basis, $B_1(t), \ldots, B_{K_1}(t)$, (resp. $\mathcal{B}_1(t), \ldots, \mathcal{B}_{K_2}(t)$) of order q_1 (resp. q_2) with k_1 (resp. k_2) equi-spaced interior knots in the period of interest for the expansion of the mean phenological curves (resp. the individual variations) where $K_1 = k_1 + q_1$ (resp. $K_2 = k_2 + q_2$) is the dimension of the functional space spanned by the B-splines.

Approximation to the individual responses can be written as follows

$$\rho_{ij}(t) \approx \sum_{k=1}^{K_1} \theta_{k,j} B_k(t) + \sum_{s=1}^{K_2} \delta_{s,j}^i \mathcal{B}_s(t), \tag{6}$$

separating the fixed effects, $\theta_{k,j}$, from the random effects $\delta_{s,j}^i$ which are supposed to be centered. Going back to the mixed pixels trajectories, we get

the formulation for the aggregated data

$$X_i(t_\nu) \approx \sum_{j=1}^{J} \pi_{ij} \sum_{k=1}^{K_1} \theta_{k,j} B_k(t_\nu) + \sum_{j=1}^{J} \pi_{ij} \sum_{s=1}^{K_2} \delta_{s,j}^i \mathcal{B}_s(t_\nu) + \varepsilon_{i,t_\nu}, \quad (7)$$

for $\nu = 1, \ldots, p$ and $i = 1, \ldots, n$. Denoting by $\gamma_j^{s,\ell} = \mathrm{Cov}(\delta_{s,j}^i, \delta_{\ell,j}^i)$, this can also be written in a matrix way as follows

$$\mathbb{E}\left(\mathbf{X}_i | \boldsymbol{\pi}_i\right) = \mathbf{B}\boldsymbol{\theta}\boldsymbol{\pi}_i \quad (8)$$

$$\mathrm{Var}\left(\mathbf{X}_i | \boldsymbol{\pi}_i\right) = \sigma^2 \mathbf{I}_p + \sum_{j=1}^{J} \pi_{ij}^2 \sum_{s,\ell=1}^{K_2} \gamma_j^{s,\ell} \boldsymbol{\mathcal{B}}_s \boldsymbol{\mathcal{B}}_\ell' \quad (9)$$

where $\mathbf{X}_i = (X_i(t_1), \ldots, X_i(t_p))$, $\boldsymbol{\theta}$ is the matrix $K_1 \times J$ whose elements are $[\boldsymbol{\theta}]_{k,j} = \theta_{k,j}$, $\mathbf{B}$ (resp. $\boldsymbol{\mathcal{B}}$) is the matrix $p \times K_1$ (resp. $p \times K_2$) whose elements are $[\mathbf{B}]_{\nu,k} = B_k(t_\nu)$ (resp. $[\boldsymbol{\mathcal{B}}]_{\nu,k} = \mathcal{B}_k(t_\nu)$), $\mathbf{B}_k = (B_k(t_1), \ldots, B_k(t_p))'$ and $\boldsymbol{\mathcal{B}}_s = (\mathcal{B}_s(t_1), \ldots, \mathcal{B}_s(t_p))'$.

Note that (9) does not assume that $\delta_{s,j}^i$ and $\delta_{s',j}^i$ are independent for $s \neq s'$ but we assume that there is no correlation between different crops.

Remark 1 *Such a B-splines decomposition is still valid even if the pixels are not exactly observed at the same instants which is the case when we have S10 synthesis (see e.g. Duchemin & Maisongrande 2002, Maisongrande et al. 2004). To remain valid, we only have to assume that there is at least one time measurement between two adjacent interior knots which is generally true if the number of knots is not too high. Then, one can consider vectors* $\mathbf{B}_{k,i}$ *and* $\boldsymbol{\mathcal{B}}_{s,i}$ *that depend on* i *without modifying the estimation procedure described below.*

3.2 Likelihood function

At this stage, let us introduce the following notation. Denote by $\mathbf{V}_i$ the variance of the digitized trajectory $\mathbf{X}_i$, defined in (9),

$$\mathbf{V}_i = \sigma^2 \mathbf{I}_p + \sum_{j=1}^{J} \pi_{ij}^2 \boldsymbol{\mathcal{B}} \tilde{\boldsymbol{\Gamma}}_j \boldsymbol{\mathcal{B}}' \quad (10)$$

where $\tilde{\boldsymbol{\Gamma}}_j$ is a matrix $K_2 \times K_2$ whose elements are $[\tilde{\boldsymbol{\Gamma}}_j]_{s,l} = \gamma_j^{s,l}$.

The log-likelihood, equals, up to a constant

$$\mathcal{L} = -\frac{1}{2}\left(\sum_{i=1}^{n} \log|\mathbf{V}_i| + \sum_{i=1}^{n} \left(\mathbf{X}_i - \mathbf{B}\boldsymbol{\theta}\boldsymbol{\pi}_i\right)' \mathbf{V}_i^{-1} \left(\mathbf{X}_i - \mathbf{B}\boldsymbol{\theta}\boldsymbol{\pi}_i\right)\right) \quad (11)$$

and the parameters to be estimated are σ^2, the $K_1 \times J$ matrix $\boldsymbol{\theta}$ and the J covariance matrices $\tilde{\boldsymbol{\Gamma}}_j$ whose sizes are $K_2 \times K_2$.

3.3 The optimisation algorithm

The estimation procedure proposed here is based on combination of the backfitting algorithm and a kind of EM algorithm (Laird and Ware, 1982), called ECME which is known to converge faster than the classical EM algorithm (McLachlan and Krishnan, 1997). Let us also notice that one major advantage of this approach compared to direct optimization procedures is that the estimated covariance matrices are automatically non negative.

One reasonable approach to maximize (11) is to consider an alternating procedure for linear mixed models and conditional variance estimation. The steps of the algorithm are the following ones

1. Initialization : get $\widehat{\boldsymbol{\theta}}^0$ by classical least squares (see Cardot *et. al.*, 2003).
2. Determine an estimator of the variance components $\tilde{\boldsymbol{\Gamma}}_j$ and σ^2 with the ECME step (see below).
3. Maximize the likelihood according to $\boldsymbol{\theta}$, $\widehat{\tilde{\boldsymbol{\Gamma}}_{\boldsymbol{j}}}$ and $\widehat{\sigma}^2$ being obtained at previous step. This step is equivalent to a weighted least squares minimization.
4. Iterate steps 2 and 3 until convergence. The algorithm is stopped when the variations of $\widehat{\sigma}^2$ are less than 0.001.

Once the algorithm has converged, we can deduce estimation of the phenological curves for each instant t,

$$\widehat{\rho}_j(t) \quad = \quad \sum_{k=1}^{K_1} \widehat{\theta}_{k,j} B_k(t) \tag{12}$$

as well as the covariance functions

$$\widehat{\gamma}_j(s,t) = \boldsymbol{\mathcal{B}}'(s)\widehat{\tilde{\boldsymbol{\Gamma}}_{\boldsymbol{j}}}\boldsymbol{\mathcal{B}}(t) \tag{13}$$

where $\boldsymbol{\mathcal{B}}(t) = (\mathcal{B}_1(t), \ldots, \mathcal{B}_{K_2}(t))'$.

These steps are described in details in the following sections.

3.3.1 Estimating the variance components with ECME

Let us denote by $\boldsymbol{\delta}_j^i = (\delta_{1,j}^i, \ldots, \delta_{K_2,j}^i)'$ the vector individual components.

Assuming that we have estimators (obtained during previous iteration of the algorithm) for the individual covariance matrices, $\widehat{\mathbf{V}}_i$, we can deduce the conditional expectations for the individual components $\widehat{\boldsymbol{\delta}}_j^i = \mathbb{E}\left(\boldsymbol{\delta}_j^i \mid \mathbf{X}_i\right)$ as

well as $\widehat{\boldsymbol{\varepsilon}}_i = \mathbb{E}\left(\boldsymbol{\varepsilon}_i \mid \mathbf{X}_i\right)$ using the BLUP formula,

$$\widehat{\boldsymbol{\delta}}_j^i = \pi_{ij}\tilde{\boldsymbol{\Gamma}}_j \boldsymbol{\mathcal{B}}'\widehat{\mathbf{V}}_i^{-1}\left(\mathbf{X}_i - \sum_{j=1}^{J}\pi_{ij}\mathbf{B}\widehat{\boldsymbol{\theta}}_j\right), \tag{14}$$

$$\widehat{\boldsymbol{\varepsilon}}_i = \mathbf{Y}_i - \sum_{j=1}^{J}\pi_{ij}\left(\mathbf{B}\widehat{\boldsymbol{\theta}}_j + \boldsymbol{\mathcal{B}}\widehat{\boldsymbol{\delta}}_j^i\right). \tag{15}$$

With these expressions we can get estimates of the variance components

$$\begin{aligned} n\,\widehat{\tilde{\boldsymbol{\Gamma}}}_j &= \mathbb{E}\left(\sum_{i=1}^{n}\widehat{\boldsymbol{\delta}}_j^i(\widehat{\boldsymbol{\delta}}_j^i)' \mid \mathbf{X}_i\right) \\ &= \sum_{i=1}^{n}\left\{\widehat{\boldsymbol{\delta}}_j^i(\widehat{\boldsymbol{\delta}}_j^i)' + \mathrm{Var}\left(\boldsymbol{\delta}_j^i \mid \mathbf{X}_i\right)\right\}. \end{aligned} \tag{16}$$

The variance σ^2 of the noise is estimated by

$$\begin{aligned} np\,\widehat{\sigma}^2 &= \mathbb{E}\left(\sum_{i=1}^{n}\boldsymbol{\varepsilon}_i'\boldsymbol{\varepsilon}_i \mid \mathbf{X}_i, \widehat{\tilde{\boldsymbol{\Gamma}}}_1, \ldots, \widehat{\tilde{\boldsymbol{\Gamma}}}_p\right) \\ &= \sum_{i=1}^{n}\left\{\widehat{\boldsymbol{\varepsilon}}_i'\widehat{\boldsymbol{\varepsilon}}_i + \mathrm{tr}\ \mathrm{Var}\left(\boldsymbol{\varepsilon}_i \mid \mathbf{X}_i\right)\right\}. \end{aligned} \tag{17}$$

Formulas for the expected conditional variances are given in McLachlan and Krishnan (1997).

3.3.2 A backfitting algorithm for weighted least squares iterations

Let us notice that the least squares criterion corresponding to step 0 and step 3 in the previous algorithm can also be expressed in a matrix way as follows :

$$\min_{\boldsymbol{\theta}}\ \varphi(\boldsymbol{\theta}) = \sum_{i=1}^{n}\left\|\mathbf{X}_i - \sum_{j=1}^{J}\pi_{ij}\mathbf{B}\widehat{\boldsymbol{\theta}}_j\right\|^2_{\mathbf{V}_i^{-1}}, \tag{18}$$

where $\|\mathbf{X}\|^2_{\mathbf{V}_i^{-1}} = \mathbf{X}'\mathbf{V}_i^{-1}\mathbf{X}$. Then, finding the roots of the set of score equations

$$\left.\frac{\partial\varphi(\boldsymbol{\theta})}{\partial\boldsymbol{\theta}_j}\right|_{\boldsymbol{\theta}=\widehat{\boldsymbol{\theta}}} = \mathbf{0}, \quad j = 1, \ldots, J, \tag{19}$$

is equivalent to solve the problem according to $\boldsymbol{\theta}_1, \ldots, \boldsymbol{\theta}_J$

$$\sum_{j'=1}^{J}\left(\sum_{i=1}^{n}\pi_{ij}\pi_{ij'}\mathbf{B}'\mathbf{V}_i^{-1}\mathbf{B}\right)\boldsymbol{\theta}_{j'} = \sum_{i=1}^{n}\pi_{ij}\mathbf{B}'\mathbf{V}_i^{-1}\mathbf{X}_i, \quad j = 1, \ldots, J. \tag{20}$$

Solving this system of equations can be done rather rapidly by blocks with the backfitting algorithm (Hastie & Tibshirani, 1990).

4 A simulation study

Before applying our method to real data sets we perform a brief simulation study in order to evaluate the effectiveness of the estimation procedure.

We have simulated n aggregated trajectories

$$X_i(t) = \sum_{j=1}^{J} \pi_{ij}\ \rho_{ij}(t) + \epsilon_{i,t}$$

with

- $i = 1, \ldots, n = 1000$ pixels
- $j = 1, \ldots, J = 3$ classes, $\quad \pi_{ij} \sim$ uniform law in $[0, 1]$ (normalised)
  $\rho_1(t) = 5\exp(-(t-0.5)^2/0.1), \quad \gamma_1(s,t) = \exp(-|s-t|),$
  $\rho_2(t) = 6\exp(-(t-0.4)^2/0.02), \quad \gamma_2(s,t) = (1+4(t-s)^2)^{-2}$
  $\rho_3(t) = 6\exp(-(t-0.7)^2/0.05), \quad \gamma_3(s,t) = (1+4(t-s)^2)^{-4}$
- $p = 40$ instants sorted in ascending order, $t_1 \leq \ldots \leq t_p$, and drawn from a Uniform distribution in $[0, 1]$.
- $\mathrm{Var}(\epsilon_{i,t}) = \sigma^2 = 0.05$

The mean response curves ρ_1, ρ_2 and ρ_3 can be understood as classical phenological curves (not scaled in this simulation study) with a growing period and then a decreasing one. They differ each other from the growing rates and the instants they reach their maximum.

In the estimation procedure, we have chosen $k_1 = k_2 = 5$ interior knots and order $q_1 = q_2 = 3$ so that $K_1 = K_2 = 8$ for the B-splines functions, allowing for a certain flexibility without needing to estimate too many parameters. We also consider other basis, allowing the number of interior knots to vary : it appeared, provided this number is not too low (less than 4) and not too high (more than 10), the results are quite the same. The algorithm, coded in R, is fast and takes less than one minute to converge with $1 + 3 \times 8 + 3 \times 8 \times 9/2 = 133$ parameters to estimate.

Disaggregation

We have drawn in Figure 3 a realisation of X and the estimated mean response curves defined in (12). We clearly see that the B-splines expansion give very accurate estimations to the mean behavior of the different themes. If we study the variance components, the conclusion are quite the same. The

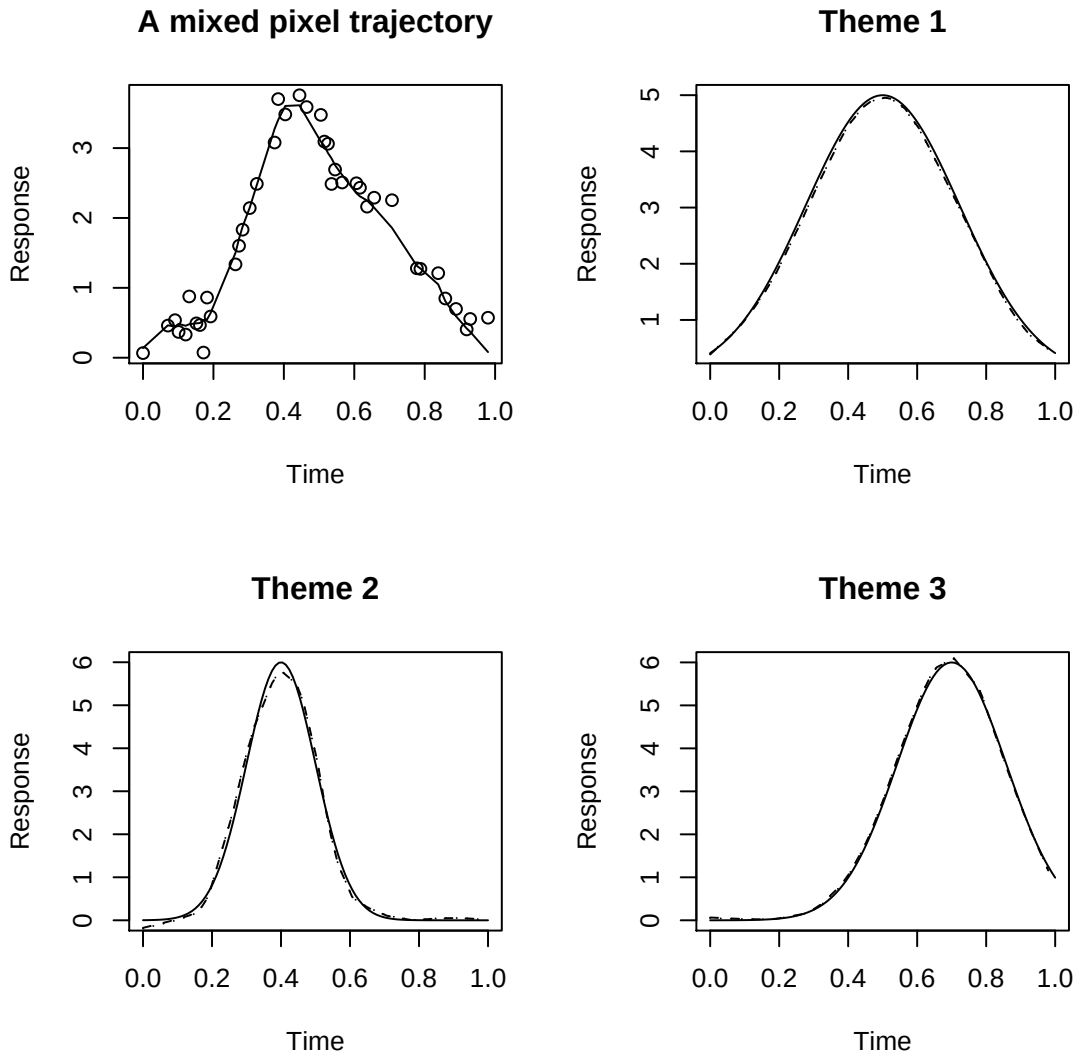

FIG. 3 – An example of simulated mixed pixel trajectory (plain line) and its noisy discretized observation (circles). True (plain line) and estimated (dotted line) mean response curves of the three different classes.

estimator $\widehat{\sigma}^2 = 0.048$ whereas the true value is 0.05. Considering now the loss criterion

$$\frac{\sum_{\ell,\ell'}^{p} \left(\widehat{\gamma}_j(t_\ell, t_{\ell'}) - \gamma_j(t_\ell, t_{\ell'})\right)^2}{\sum_{\ell,\ell'}^{p} \gamma_j(t_\ell, t_{\ell'})^2}$$

to evaluate the skill of the covariance term estimation, we get an error of about 0.06 for $\widehat{\gamma}_1$, 0.04 for $\widehat{\gamma}_2$, and 0.08 for $\widehat{\gamma}_3$, which means that we have obtained rather good approximations to the true covariance functions.

Let us look now, in Figure 4, at the estimation of the local responses, $\widehat{\rho}_{ij}$ obtained thanks to the BLUP formula. We first notice that if the proportion of the theme (theme 3 here with $\pi_{i3} = 0.49$) is sufficiently high, then there is an important gain in considering a mixed effects model and our estimators are able to capture rather well the variations from the mean response curve. On the other hand, if the proportion of the theme is not high enough (theme 1, with $\pi_{i3} = 0.23$), that is to say its contribution to the aggregated curve X_i is too low, then the individual curves is very similar to the mean response of the theme and there is no real gain in considering a mixed effects model for estimating individual trajectories.

Temporal interpolation

To study the sensitivity of the quality of interpolation to the number ℓ of high resolution points, we consider a number ℓ of observed high resolution images varying from $\ell = 3$ to $\ell = 9$, the ℓ instants being equispaced in $[0, 1]$. We compare 4 interpolation approaches, ordered according to an increasing level of information,

- performing a linear interpolation of the high resolution trajectories (method "lin").
- taking into account the estimated mean response curve and performing a linear interpolation of the local variation (the residuals) around this mean trajectory. This corresponds to a BLUP interpolation with a predefined covariance function (method "res").
- applying the BLUP formula (4) which takes into account both the mean phenological curve and the covariance function ("blup1").
- taking into account both the high resolution and the low resolution trajectories in the BLUP formula ("blup2").

The error is evaluated with the mean square error of approximation at the predicted points. Table 1 gives these errors when interpolating trajectories of crops belonging to theme 3. We first remark that the linear interpolation is not effective at all when the number ℓ of measurements is too low. The "res" method does not perform too badly, the information brought by

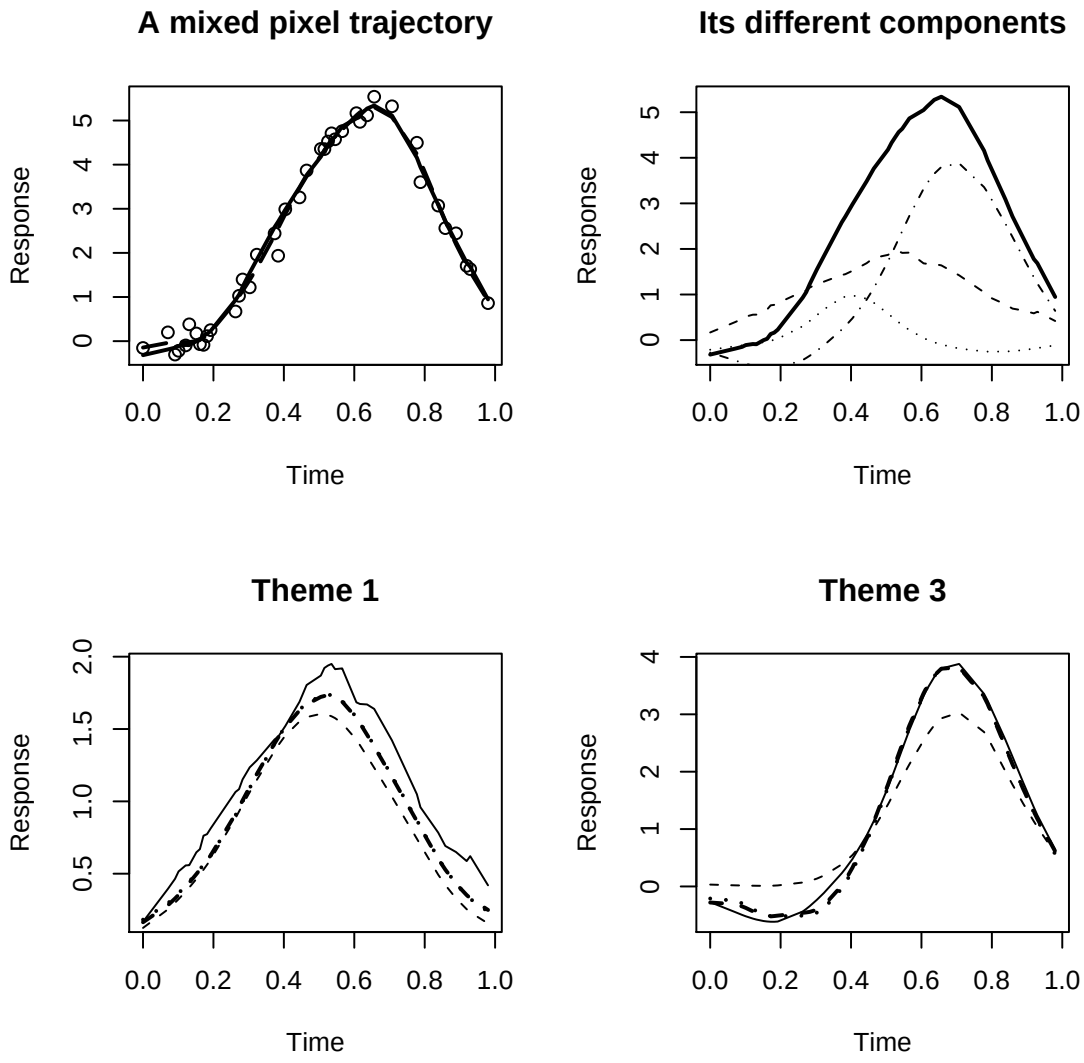

FIG. 4 – An example of simulated mixed pixel trajectory (bold line) and its noisy discretized observation (circles). The second display presents the true trajectory (bold line) the contribution of the three different themes (dotted lines). The third and fourth displays present the contribution of the first and third theme (line), whose corresponding proportions are $\pi_{i1} = 0.23$ and $\pi_{i3} = 0.49$, the estimated weighted mean response of the theme (dotted line) and the estimated individual component (bold dotted line).

MSE	3 pts	5 pts	7 pts	9 pts
lin	2.65	0.57	0.26	0.038
res	0.24	0.081	0.051	0.011
blup1	0.23	0.052	0.022	0.004
blup2	0.12	0.037	0.018	0.004

TAB. 1 – Mean Square Error (MSE) of interpolation according to the number of observed high resolution data for the four different approaches.

MSE	3 pts	5 pts	7 pts	9 pts
lin	2.65	0.56	0.26	**0.038**
res	0.25	0.082	**0.052**	0.011
blup1	0.24	**0.052**	0.021	0.004
blup2	**0.051**	0.024	0.014	0.004

TAB. 2 – Mean Square Error (MSE) of interpolation according to the number of observed high resolution data for the four different approaches when considering mixed pixels containing more than 40 % of theme 3.

the mean phenological curve telling what are the most important variations of the crop. Nevertheless, as the temporal information increases, the two blup approaches get better and better, allowing to take into account smaller variations. The blup2 approach is always better and provides good interpolations even for a small number of high spatial resolution data. On the contrary, when $\ell = 9$, the two blup approaches give similar errors, meaning that coarse resolution data do not bring additional information anymore.

If we restrict now the computation of the loss criterion to the pixels containing more than 40 % of theme 3, we can see in Table 2) that the information brought by the aggregated trajectories still improve significantly the prediction error made by the blup2 method, even for a small number ℓ of high resolution data.

5 Application : the "Sud-Ouest" project

In this section, the synthetic exercice previously described is now applied to an actual remote sensing dataset. Thanks to the South-West Project (`http ://www.cesbio.ups-tlse.fr/us/sud_ouest.html`) carried on at CESBIO, we took advantage of the simultaneous availability of high and low

	Forest	Wheat	Maize	Pastures
1st axis	42 %	67 %	49 %	63 %
2nd axis	23 %	22 %	24 %	21 %
3rd axis	15 %	6 %	12 %	11 %

TAB. 3 – Explained variance by the first three eigenfunctions of the estimated covariance operators of four important "crops" in the South-Western project.

resolution time series during year 2002. Indeed, we have at our disposal 36 VEGETATION images, *i.e.* one image every 10 days (S10 synthesis see Maisongrande *et al.* 2004) as well as 10 high resolution images SPOT4/HRV (Coret et al. 2005). Within this pilot site, we have selected an area with a surface of about n =4500 km^2 in the South-Western of France. We consider the $J = 7$ most important themes in this region, which are Forest 9%, Wheat 22%, Maize 8%, Sunflower 12%, Pastures 26%, Urban 12% and "Remainding" representing 11 % of the total surface. The land use classification was made at CESBIO (Ducrot *et al.* 2004) using a classification algorithm based on multispectral and multitemporal high resolution data.

5.1 Disaggregating VEGETATION data

We first calibrate, with the land use and the VEGETATION data, the random effects model to get estimates of the mean temporal profiles of the different themes (equation 12) as well as their covariance functions (equation 13) using the algorithm described previously. The estimated mean phenological curves of the themes "Forest", "Wheat", "Maize" and "Pastures" are drawn in Figure (5) where we can clearly see that the responses along time of the different types of vegetation vary in their intensities but also in their variabilities. For instance, the theme "Pastures" seems to have larger variations of its variability, from one location to another, than other crops. To study in details the largest mode of variations of these classes, we have performed the spectral analysis, or functional PCA, of the estimated covariance functions. The variance explained by the first three principal components are given in Table 3. We can notice that mainly all the variability of these crops, that is to say more than 80 % of the total variations, is captured by approximating the individual trajectories in a two dimensional space for "wheat" and "Pastures" and a three dimensional space for the themes "Forest" and "Maize".

We have also drawn in Figure (6) the first two eigenfunctions for these

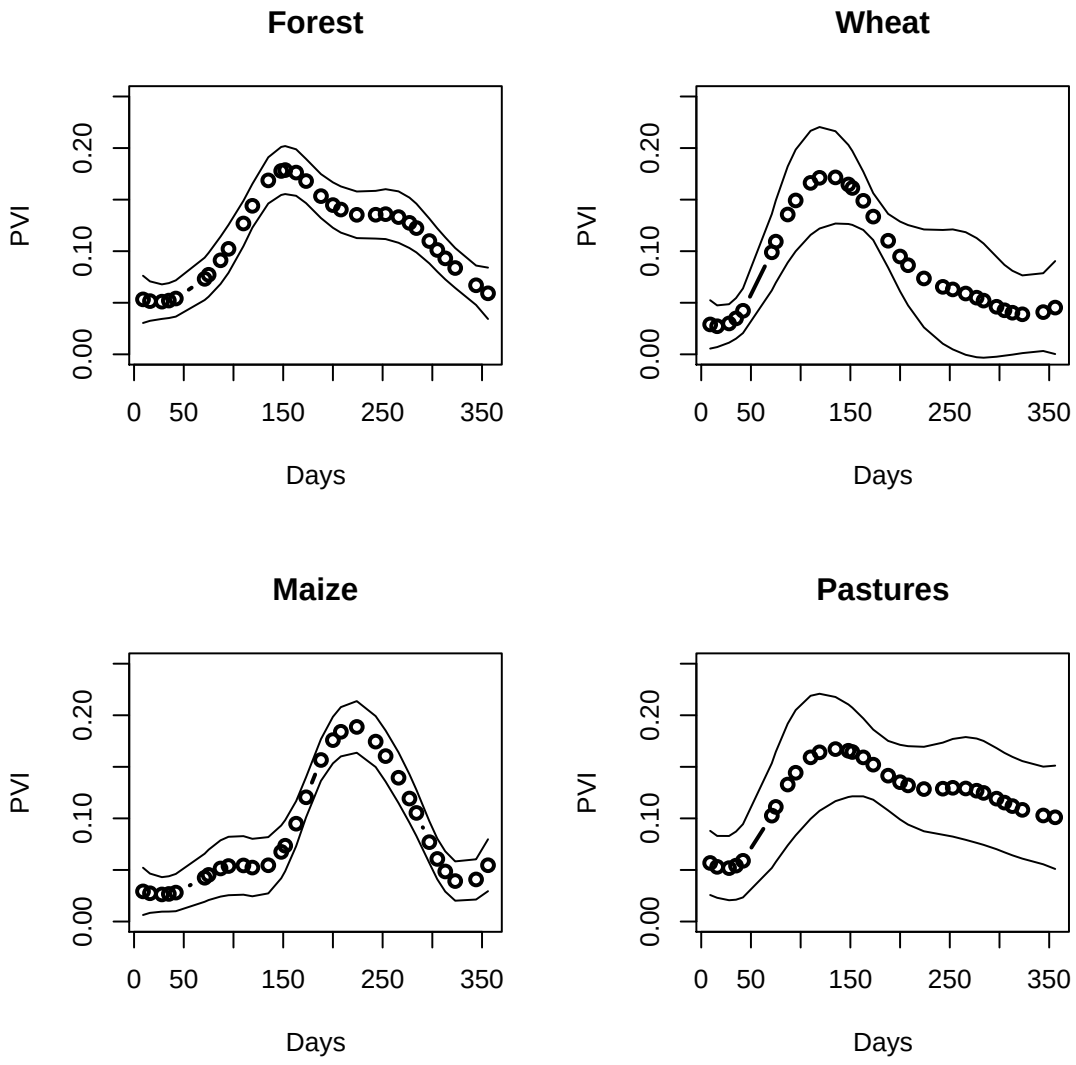

FIG. 5 – Estimated mean phenological curves (circles) with the PVI during year 2002 with VEGETATION data for the themes "Forest", "Wheat", "Maize" and "Pastures". We have added ± two times the instantaneous standard deviations in order to characterize the main instants in time of variability (plain lines).

MSE	All pixels	Surf $\geq$40%
lin	6.64	4.68
res	4.68	2.85
blup1	4.78	2.08
blup2	4.09	2.05

TAB. 4 – Interpolation errors of the PVI index for the SPOT4 high resolution pixels containing "Wheat" crops as well as those for which the "Wheat" plots represent more than 40 % of the total surface.

crops. This also clearly points out that the principal modes of variability can be very different from one crop to another. This also tends to improve the ability of the BLUP formula to discriminate between the contributions of the different crops inside a mixed pixel.

5.2 Temporal interpolation of SPOT4/HRVIR data

In the same area, high resolution images were available at a few number of time instants, $\tau_1 < \ldots < \tau_{10}$. In order to evaluate the ability of the mixed effects approach to get approximations to high resolution trajectories, we have supposed that we have observed only 4 High Resolution images (at the dates $\tau_1, \tau_3, \tau_5, \tau_8$) and we want to estimate the evolution for the 6 other dates. The mean square errors of prediction, with the PVI index for the theme "Wheat", are presented in Table 4.

We first notice that taking into account VEGETATION data (medium resolution trajectories) allows us to get better temporal interpolation of high resolution data. Indeed, the "lin" method performs poorly compared to the approaches incorporating VEGETATION data. The gain can be rather important, the error being divided by two compared to the "lin" method, when considering pixels containing more 40 % of wheat crops. Nevetheless, even if the methods based on the BLUP give better predictions, the main improvement in the interpolation seems to be due to the knowledge of the mean temporal response in the area under study.

Many factors can explain this lack of improvement and the main one seems to be a *calibration problem*, meaning that the reflectances of the two different sensors are not exactly calibrated the same way and thus the temporal evolution of medium resolution pixels is not as useful as it could be for interpolating high resolution ones. This is clearly seen in Figure 7 where we have drawn the mean phenological curves of four different crops according

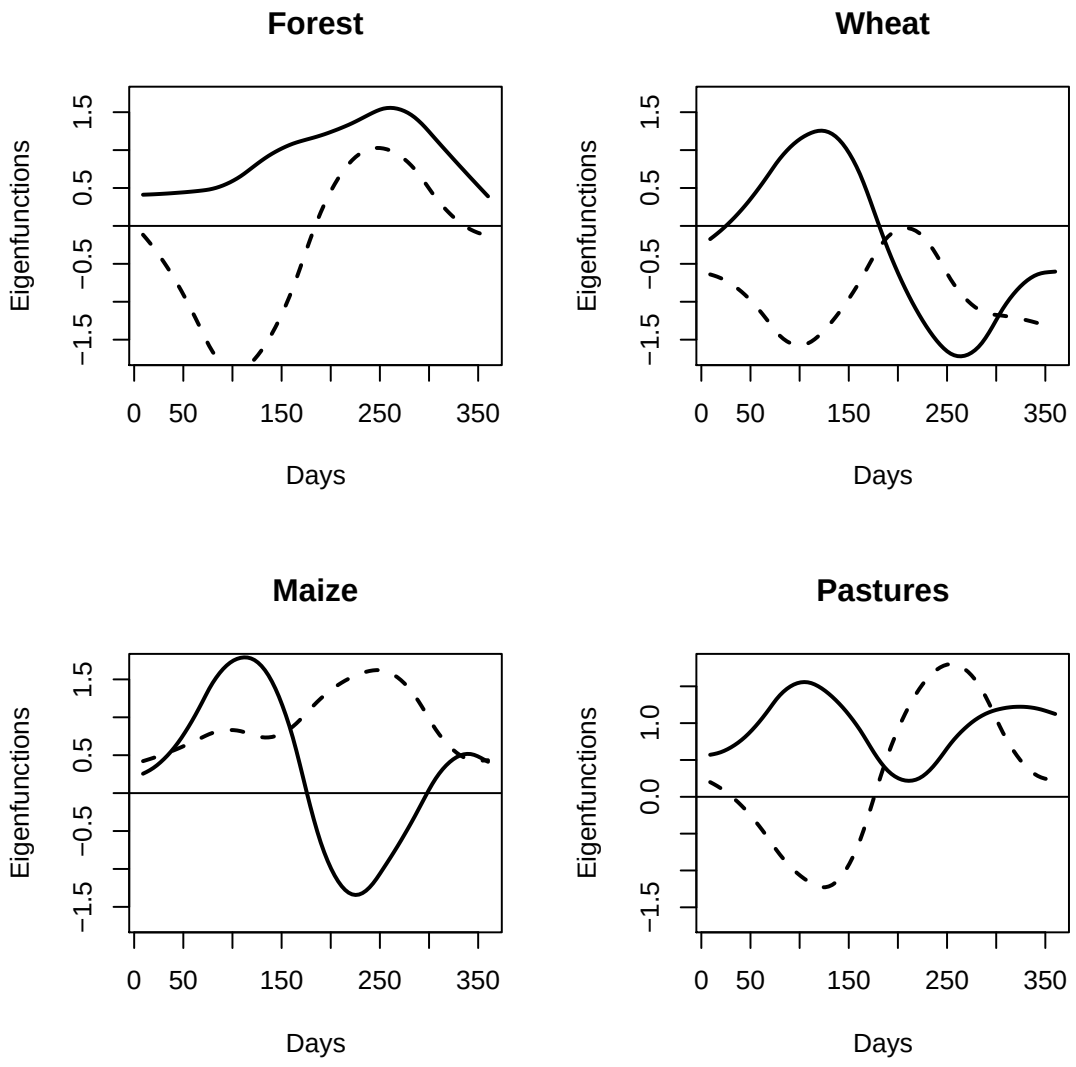

FIG. 6 – Estimated first two eigenfunctions during year 2002 with VEGETATION data for the themes "Forest", "Wheat", "Maize" and "Pastures". The first eigenfunction is drawn in plain lines whereas the second one is in dotted lines.

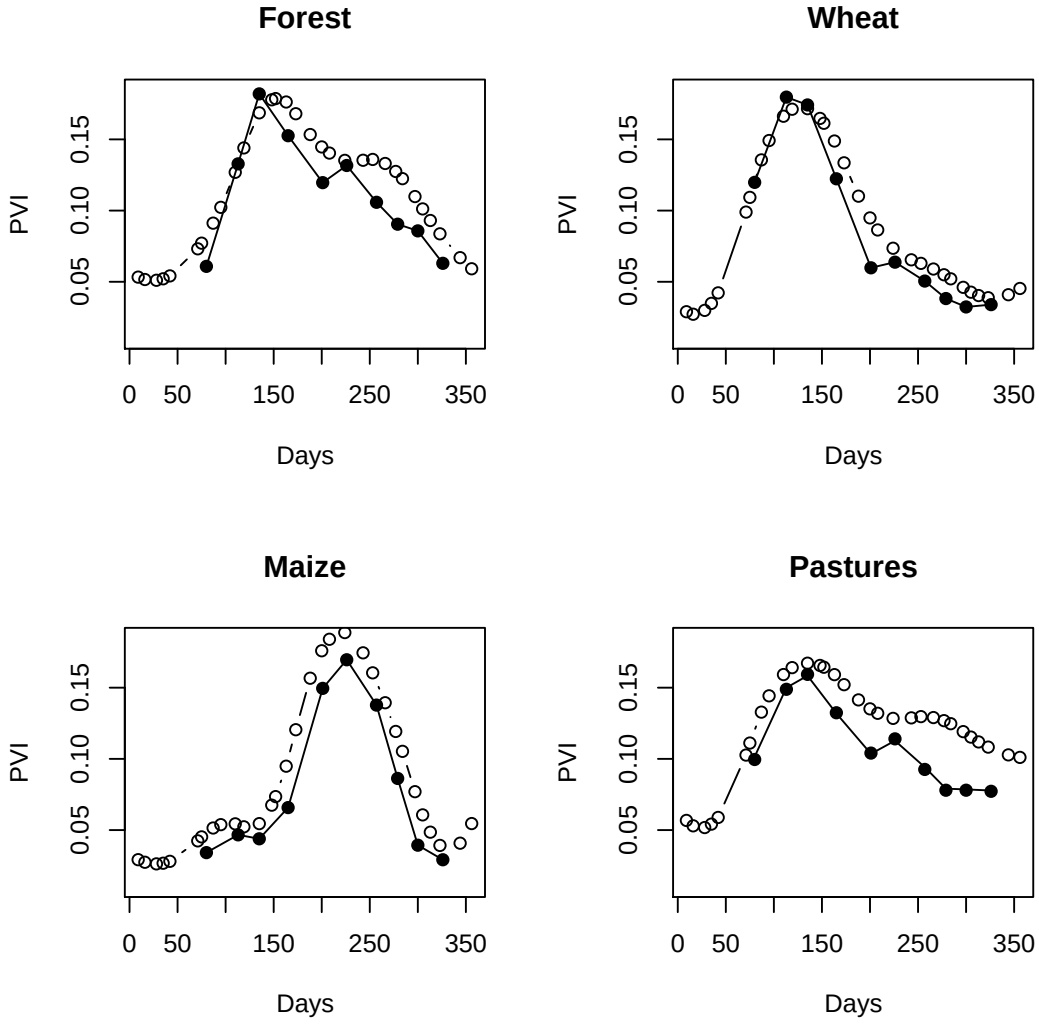

FIG. 7 – Comparison of the estimations of phenological curves according to the resolution of the sensor, small circles for SPOT4/VEGETATION, lines with black points for SPOT4/HRVIR.

to the two spatial resolutions for the PVI index.

6 Concluding remarks

Downscaling reflectances of mixed pixels is an important but difficult issue in remote sensing, allowing to deduce with physical models many useful local information such as water demand, soil moisture, crops development, fine land use classification, ... Unfortunately, when using satellite data, one often has to cope with a compromise between resolution and time frequency. The low resolution imagery is cheap and frequent but its drawback is the aggregative character of the radiometric information it contains.

We propose here a natural approach for disaggregation based on mixed effects models for longitudinal data able to handle huge samples with many time measurements. We have seen in the simulation study that the proposed algorithm is rather efficient, leading to accurate estimation with a fast algorithm. We also noticed that the proposed approach appears to be a very interesting candidate for downscaling classes whose contribution to the total surface is not too small.

This statistical approach of desaggregation can also be helpfull. Indeed, our model can address the combination of Low and High Resolution (information brought by both types of sensors) making thus possible studies necessary to the dimentioning of future satellite missions that could combine the two types of sensors. Space Agencies and satellite makers could for example evaluate the number and type of sensors that will have to operate simultaneously in order to ensure a su ?ciently frequent crop monitoring, at a specified level of precision.

More generally, mixed effects models are widely used in medicine and economy (Kneip *et al.*, 2003), allowing to describe individual characteristics with random parameters statistical models. Nowadays it is frequent to have longitudinal data/functional data with many individuals and many time measurements. Our approach which can also incorporate effectively the effects of a relatively large number of covariates seems to be a good candidate for such studies.

Sensitivity to inter-resolution consistency

The simulation study clearly shows that taking into account simultaneously the information brought by sensors with different resolutions can lead to considerable potential gain in temporal interpolation of High Resolution data. Nevertheless, our work points out the need for an as good as

possible HR layer versus LR layer juxtaposition when one wants to take advantage of the complementarity between the 2 types of data. The required consistency principally depends on various factors such as : sensors intercalibration, accuracy of each layer georeferecing, projections consistency, and also neighbourhood effects (between adjacent pixels) which present patterns that are resolution dependent. Although a particular attention was paid on these different points, residual artefacts (principally geometric) might persist and explain a part of the difference between the synthetic and the real data exercise. This issue is beyond the scope of the paper but deserves further attention. For example, we logically expect a gain of consistency when reducing the resolution gap when considering 250 m resolution data (*e.g.* MODIS sensor) instead of the kilometric pixels of SPOT/VEGETATION.

Sensitivity to spatial correlation

Besides remote sensing considerations, another point of interest is the determination of the domain of validity of such an aggregation model when there are spatial correlations between the temporal responses of a particular crop.

The ideal case for the model to be valid is when there is no variation within a mixed pixel, meaning that all the variations of the responses of different crops are "inter" mixed pixel variations. On the contrary, the worst case would be when all the variability is concentrated within coarse resolution pixels, meaning that we have a kind of "fractal" property.

If we assume that the spatial correlation is very large for very close neighbours and low for far ones, which is a realistic assumption for crops, we can suppose that we are not too far from the ideal case. Nevertheless this needs to be quantified and deserves further investigations. Then, one interesting question is what would be the best spatial resolution for disaggregation when observing mixed pixels and thus how sensors should be calibrated ?

Extension to non-linear indices

Another interesting issue is the extension to nonlinear indices such as the $NDVI$ index which is a non-linear combination of the responses in the RED and Near Infra Red (Tucker, 1979). This index is widely used in the remote sensing community because it can give a good measure of the state of a crop and it has certain robustness properties. In order to get local estimation of this index, one has to extend our random effect model and consider a multivariate response disaggregation model, with outputs $RED(t)$ and $NIR(t)$, and then perform a Taylor expansion of this index.

Applying the BLUP formula to this linear approximation allows to get local estimations of the $NDVI$. We are working on this topic but this is beyond the scope of this paper.

Acknowledgements : We would like to thank all the participants to the working group "Changement d'échelle" in Toulouse for fruitful discussions. We would like to thank G. Dedieu for allowing us to illustrate the method with the "Sud-Ouest" Project data.

Références

[1] Cardot, H., Faivre, R. and Goulard, M. (2003). Functional approaches for predicting land use with the temporal evolution of coarse resolution remote sensing data. *J. of Applied Statistics*, **30**, 1185-1999.

[2] Cardot, H., Faivre, R. and Maisongrande, P. (2004). Random Effects Varying Time Regression Models : Application to Remote Sensing. *Compstat 2004 proceedings* ed. J. Antoch, Physica-Verlag, 777-784.

[3] Coret L., P. Maisongrande, A.A. Boone, A. Lobo Aleu, G. Dedieu, P. Gouaux (2005). Assessing impacts of the 2003 Hot and Dry Spell with SPOT HRVIR Images Time Series over South-Western France. *International Journal of Remote Sensing*, in press.

[4] Déjean S., Faivre, R. and Goulard, M. (2002). Modèle non linéaire à paramètres aléatoires de la dynamique de cultures observées par télédétection : comparaison de deux procédures d'estimation. *J. Soc. Française De Statist.*, **143**, 205-213.

[5] Dierckx, P. (1993). *Curve and Surface Fitting with Splines.* Clarendon Press, Oxford.

[6] Diggle, P. J., Liang, K-Y. and Scott, S. L. (1994). *Analysis of longitudinal data.* Oxford University Press.

[7] Duchemin, B., and Ph. Maisongrande (2002). Normalisation of directional effects in 10-day global syntheses derived from VEGETATION/SPOT. I Investigation of concepts based on simulation. *Remote Sensing of Environment*, **81**, 90-100.

[8] Duchemin, B., B. Berthelot B, G. Dedieu, M. Leroy, P. Maisongrande, (2002). Normalisation of directional effects in 10-day global syntheses derived from VEGETATION/SPOT : II. Validation of an operational method on actual data sets. *Remote Sensing of Environment*, **81**, 101-113.

[9] Ducrot, D, Gouaux, P. (2004). Caractérisation des agro-systèmes de la plaine alluviale de la Garonne et des coteaux du Gers, mise en évidence de leurs changements au cours des dix dernires années. *Colloque Société Française Economie Rurale, Systèmes de production : performances, évolution, perspectives*, Lille.

[10] Faivre, R. and Fischer A., (1997). Predicting crop reflectances using satellite data observing mixed pixels. *Journal of Agricultural, Biological and Environmental Statistics*, **2**, 87-107.

[11] Foody, G.M. and Cox, D.P. (1994). Sub-pixel land cover composition estimation using a linear mixture model and fuzzy membership functions. *International Journal of Remote Sensing*, **15**, 619-631.

[12] Hastie, T. and Tibshirani, R. (1990). *Generalized Additive Models.* London, Chapman & Hall.

[13] Hoover, D.R., Rice, J.A., Wu, C.O. and Yang, L.P. (1998). Nonparametric smoothing estimates of time-varying coefficient models with longitudinal data. *Biometrika*, **85**, 809-822.

[14] Kneip, A., Sickles, R. and Song, W. (2003). On estimating the mixed effects model. *Preprint.*

[15] Laird, N. and Ware, J. (1982). Random-Effects Models for Longitudinal Data. *Biometrics*, **38**, 963-974.

[16] McLachlan, G. and Krishnan, T. (1997). *The EM Algorithm and Extensions.* John Wiley & Sons.

[17] Maisongrande, P., B. Duchemin, G. Dedieu, (2004). VEGETATION/SPOT - An Operational Mission for the Earth Monitoring : Presentation of New Standard Products. *International Journal of Remote Sensing*, **25**, 9-14.

[18] Merlin, O, Chehbouni, A.G.,Kerr, Y. H., Njoku, E.G., and D. Entekhabi (2005). A Combined Modeling and Multi-Spectral/Multi-Resolution Remote Sensing Approach for Disaggregation of Surface Soil Moisture : Application to SMOS Configuration. *IEEE Geoscience and Remote Sensing*, **43**, 2036-2050. ?

[19] Ramsay, J., Silverman, B.W. (2005). *Functional Data Analysis.* Springer-Verlag, 2nd ed..

[20] Rice, J. (2004). Functional and longitudinal data analysis : Perspectives on smoothing. *Statistica Sinica*, **14**, 631-647.

[21] Rice, J. and Wu, C. (2001). Nonparametric mixed effects models for unequally sampled noisy curves. *Biometrics*, **57**, 253-259.

[22] Richards J.A., Jia, X. (2005). *Remote Sensing Digital Image Analysis : An Introduction*. Springer-Verlag, Berlin, 4th ed..

[23] Richardson A.J. and Wiegang, C.L., (1977). Distinguishing Vegetation from Soil Background Information. *Photogrammetric Engineering and Remote Sensing*, **43**, 1541-1552.

[24] Robinson, G.K. (1991). That BLUP is a good thing : The estimation of random effects. *Statistical Science*, **6**, 15-51.

[25] Tucker, C.J., (1979). Red and Photographic Infrared Linear Combinations for Monitoring Vegetation. *Remote Sensing of Environment*, **8**, 127-150.

[26] Wu, H., and Liang, H. (2004). Backfitting Random Varying-Coefficient Models with Time-Dependent Smoothing Covariates. *Scand. J. of Statist.*, **31**, 3-19.